Hindawi Publishing Corporation
Journal of Nanomaterials
Volume 2015, Article ID 470297, 9 pages
http://dx.doi.org/10.1155/2015/470297

Research Article

The Effect of Oxygen-Plasma Treated Graphene Nanoplatelets upon the Properties of Multiwalled Carbon Nanotube and Polycarbonate Hybrid Nanocomposites Used for Electrostatic Dissipative Applications

Akkachai Poosala,[1] Kittipong Hrimchum,[2] Darunee Aussawasathien,[2] and Duanghathai Pentrakoon[3]

[1]*Technopreneurship and Innovation Management, Graduate School, Chulalongkorn University, Bangkok 10330, Thailand*
[2]*Plastics Technology Lab, Polymer Research Unit, National Metal and Materials Technology Center, Pathum Thani 12120, Thailand*
[3]*Department of Materials Science, Faculty of Science, Chulalongkorn University, Bangkok 10330, Thailand*

Correspondence should be addressed to Darunee Aussawasathien; daruneea@mtec.or.th and Duanghathai Pentrakoon; duanghat@yahoo.com

Received 13 November 2014; Revised 5 January 2015; Accepted 5 January 2015

Academic Editor: Stefan I. Voicu

Oxygen-plasma treated graphene nanoplatelet (OGNP), multiwalled carbon nanotube (MWCNT) and polycarbonate (PC) hybrid nanocomposites were prepared via a melting process using a twin-screw extruder. The contents of the OGNPs were in the range of 0.0 to 5.0 parts per hundred resin (phr), whilst the dosage of MWCNTs was kept at a constant of 2.0 wt%. Nanocomposites containing 2.0 wt% of MWCNTs and mixtures of 2.0 wt% of MWCNTs at 1.5 to 5.0 phr of OGNPs had tribocharged voltages, surface resistivities, and decay times, all within the electrostatic discharge (ESD) specification. The X-ray diffraction (XRD) and scanning electron microscopy (SEM) results revealed that the OGNPs slightly intercalated and distributed also within the PC matrix. The glass transition temperature (T_g) and heat capacity jump, at the glass transition stages of nanocomposite, slightly changed, as the contents of the OGNPs increased. The melt flow index (MFI) of nanocomposites significantly decreased when MWCNTs were added to the PC resin and slightly changed as the dosage of OGNPs was increased. Tensile Young's modulus of nanocomposites tended to increase, as the elongation at break and impact strength decreased, when OGNP concentrations were increased. This research work exhibited that OGNP/MWCNT/PC hybrid nanocomposites do indeed have the potential to be used in ESD applications.

1. Introduction

Nowadays, there are susceptible problems associated with antielectrostatic discharge (ESD) properties upon the performance of electronic circuits, because ESD impacts upon most industrial products and their associated qualities. Many electronic components, especially microchips, can be damaged by ESD and therefore ESD protection of sensitive components is necessary during manufacturing, device assembly, packaging, and shipping. Electrostatic dissipating thermoplastic composites have successfully eliminated ESD failures in many applications of the electronics industry, such as injection moldable packaging and in-process trays. Various conductive fillers are currently available to material engineers, including carbon fibers (CFs), carbon black (CB), carbon nanotubes (CNTs), metallic powders, flakes or fibers, and glass spheres or glass fibers coated with metals [1]. The conductivity of ESD composites depends not only upon the filler type and its concentrations but also upon the specific polymer matrix used and its associative generated morphology [2].

CNTs, along with a cylindrical nanostructure and graphene with a two-dimensional sheet of sp^2-hybridized carbon atoms densely packed into a honeycomb network, have distinctly different geometrical shapes and yet they have remarkable properties, such as superior thermal and mechanical properties and exceptional electronic transport

[3–8], which makes them excellent candidates as reenforcers and conducting fillers in composites. Recently, theoretical and experimental studies on polymer composites containing CNTs have been carried out [9–14]. However, the investigation on GNP-filled polymer composites has been limited [14–16]. It is well documented that the morphology of fillers has a significant effect upon composite properties [17–19]. For example, Xie et al. [14] reported that GNP-filled composites exhibit slightly lower percolation thresholds and higher electrical conductivity and thus could form conductive networks more easily than CNT-filled composites, at the same volume of fraction filler. Furthermore, the improvement of polymer/graphene nanocomposite properties has also been obtained at a very low filler load in the polymer matrix [16, 20–23]. Today, the cost of GNPs is relatively more expensive than that of CNTs and, therefore, the GNP/CNT/polymer hybrid system is alternative means to obtain nanocomposites which have balanced properties and economically effective costing.

Despite this, pristine graphene is incompatible with organic polymers and does not form homogeneous composites, because graphene has a pronounced tendency to agglomerate when within a polymer matrix [24, 25]. It has also been reported that oxidation, followed by chemical functionalization, will facilitate the dispersion and stabilize graphene to prevent such agglomeration [26, 27]. The chemical functionalization of graphene is a particularly attractive target, because it can improve the solubility and process ability, as well as enhance its interactions with organic polymers [26, 27]. However, it is a tedious, dangerous, and time consuming method, which includes environmental and human health problems. It is also reported that functionalization and associated defects may distort flat graphene into highly wrinkled sheets during thermal exfoliation [23]. Sheet wrinkling and atomistic defects upon the surface, after oxidation and pyrolysis treatments, may account for its low performance concerning its mechanical properties [28].

Since the 1960s, plasma technology has rapidly evolved into a valuable technique for engineers, concerning the enhancement of surface properties without altering the bulk composition [29]. Compared to other chemical treatment methods, plasma treatment has the advantage of shorter reaction times, involves a nonpolluting process, and provides for a wide range of functional groups, dependent upon the plasma parameters. Plasma treatment is favored for the improvement of the interfacial affinity of composites, because it only modifies the top few nanometers of the surface, uniformly, and it leaves the bulk properties of the material unchanged [30, 31]. Plasma surface activation also renders many polymers receptive to bonding agents and coatings. Oxygen is usually used as the process gas, although many plasma activations can also be carried out by simply using ambient air. Parts remain active for a few minutes and up to several months, depending upon the particular material that has been plasma treated. Oxygen plasma treatment provides various polar functional groups, such as C–O, C=O, and O=C–O upon the polymer surface, which in turn alters the surface energy of the material and enhances the interfacial adhesion [32–34].

In this present work, polymer nanocomposites along with a combination of OGNPs, MWCNTs, and PC were prepared for ESD applications. In our preliminary study, it was found that PC nanocomposites containing 2 wt% of MWCNTs had ESD properties concerning surface resistivity, tribocharge voltage, and decay times all within the specified ranges. Therefore, OGNP was utilized as a cofiller with as low contents as possible in the hybrid fill system, which contained 2 wt% of MWCNTs in order to improve the properties of PC nanocomposites. The effects of OGNP contents, distribution, and intercalation upon the thermal and mechanical properties and MFI and ESD properties were all investigated.

2. Experimental Procedure

2.1. Materials and Sample Preparation. The injection molding grade of the PC resin (Makrolon 2456) was supplied by "Bayer Material Science," Thailand. The PC/MWCNT master batch (Plasticyl PC 1501) and the OGNPs (GNPs grade 4, 99% O^+) were supplied by "Nanocyl," Belgium, and "Cheap Tubes Inc.," USA, respectively, and were used as the nanofillers. All materials were dried in a vacuum oven at 120°C for 2 h, under a pressure of 49.345×10^{-3} atm, and then manually blended in a plastic container before the melting process, using a twin-screw extruder (Lab-Tech). The contents of the OGNPs incorporated into the PC resin were controlled at 0.0, 0.5, 1.0, 1.5, 2.0, and 5.0 phr, whereas the dosages of MWCNTs were kept at a constant of 2.0 wt%. The screw diameter, screw length, and screw L/D ratio were 20 mm, 640 mm, and 32, respectively. The set-up temperature of the mixing screws was in the range of 240–290°C. In addition, the rotation of the feeding screws and mixing screws was 12 rpm and 120 rpm, respectively.

All composites were dried in a hopper at 80°C for 3 h, prior to processing. The injection molding of nanocomposites was carried out using a Fanuc Roboshot 2000i 100B reciprocating screw injection molding machine, in order to obtain required tensile and impact specimens. The plasticization unit consisted of a standard screw with a diameter of 32 mm, L/D ratio of 20/1, and a compression ratio of 4D. The temperature profiles were set at 235°C, 260°C, 290°C, and 280°C, respectively, from the hopper zone to the nozzle, and the mold temperature was set at 100°C. The screw rotation speed was set at 50 rpm. The injection speed and pressure was 20 cm^3/s and 78.95×10^{-3} atm, respectively. Specimens were kept for 24 h in a desiccator, before characterization.

2.2. Characterization. The electrical resistivity of injection-molded samples was measured according to ANSI/ESD STM11.13-2004, using a resistance meter (3M-701). The tribocharge voltage and decay times were determined based upon ESD ADV11.2-1995, using an electrostatic voltage meter (Trek-520) and a charged plate monitor system (Trek Model 150A), respectively. Five specimens were tested during each measurement. Thermogravimetric analyses (TGA) measurements were carried out using "TA Instruments" thermobalance (TGA Q500) under a nitrogen atmosphere and at a heat ratio of 20°C/min from between 25°C to 1000°C. A differential

scanning calorimeter (DSC) (Mettler Toledo, Model-DSC 822e) was used for the dynamic measurement and data analysis under N_2 flow. A heating rate of 20°C/min was applied to the samples from between 25°C and 300°C. The MFI was measured using an extrusion plastometer (Davenport model 10, Lloyd Instruments), according to ISO 1133 (ASTM D1238) at 260°C with a 0.02 kN weight. The average MFI values from ten measurements of each sample were recorded. Wide angle X-ray diffraction (WAXD) characterization was carried out using a Rigaku Model-TTRAX III X-ray diffractometer. The incidental X-ray wavelength was 1.54 Å (Cu Kα line), at 50 kV and 300 mA. Samples were scanned over different diffraction angles (2θ) ranging from 1° to 45°, with a scan speed of 0.5°/min at room temperature. The cross-sectional surface morphology of nanocomposites was characterized using SEM (JEOL, JSM-5410LV). The tensile specimens were immersed in liquid nitrogen for a few minutes, and subsequently broken along, as well as perpendicular, to the material flow direction, as per injection molding. Fractured samples were attached to a SEM stub using conducting tape and then sputter-coated with a thin layer of Au using a JEOL JEC-1200 Fine Coater at 15 mA for 120 s. The tensile properties were measured according to ASTM D638 using a universal testing machine (Instron 4502), at a crosshead speed of 5 mm/min and a test temperature of 25°C. The specimen dimensions were 12.7 mm × 165 mm × 3.2 mm ($W \times L \times T$). Young's modulus and elongation at break were determined from load-displacement curves. Izod impact tests were performed on an impact tester (Radmana model ITR 2000) based upon ASTM standard D256. The notched samples had a size of 12.7 mm × 63.5 mm × 3 mm ($W \times L \times T$), respectively.

3. Results and Discussion

3.1. X-Ray Diffraction. Figure 1 illustrates the WAXD patterns of the PC resin and OGNP/MWCNT/PC nanocomposites at different OGNP concentrations. Dispersion and orientation of OGNPs in PC nanocomposites were analysed using 2-dimensional X-ray scattering. It is clearly seen that OGNPs slightly intercalated in the PC matrix because the peak intensity of OGNPs at $2\theta = 26.4°$ firmly remained, and increased as the amount of OGNPs increased, which corresponds to the interlayer spacing of unintercalated graphite ($d = 0.34$ nm) [23]. These findings are in good agreement with the results of previous experiments and confirm the existence of graphite layers of OGNPs in polymer nanocomposites [26, 35, 36]. This may be a result of slight interaction between OGNPs and the polar groups of PC, since OGNPs prepared by oxygen plasma treatment might not have enough functional groups on the surface, such as oxygen and hydroxyl groups [37], and the gap between graphene sheets still remained narrow. Therefore, variation of the OGNP intercalation levels in nanocomposites might insignificantly improve the properties of PC nanocomposites.

3.2. Scanning Electron Micrograph. SEM images taken from fractured surfaces of OGNP/MWCNT/PC nanocomposites at different OGNP content levels are shown in Figures 2(a)–2(f). The SEM results showed MWCNT and OGNP-dispersed morphologies. MWCNTs were uniformly dispersed in the PC matrix (white spots), whereas OGNPs were not clearly dispersed and agglomerated structures were also observed (white lines and white thick sheets marked with white arrows), thus implying partial distribution of OGNPs in the PC matrix. However, it is difficult to distinguish OGNP fillers from the matrix due to the roughness of the fractured sample. Therefore, a special sample preparation technique is required in order to obtain a better contrast between OGNP fillers and the PC matrix, such as polishing and polish-plasma etching approaches. Wu and Drzal [38] showed that on a plasma etched surface, the white lines represented the cross section of the GNP fillers, and the contrast between GNP fillers and the matrix was better than a polished surface.

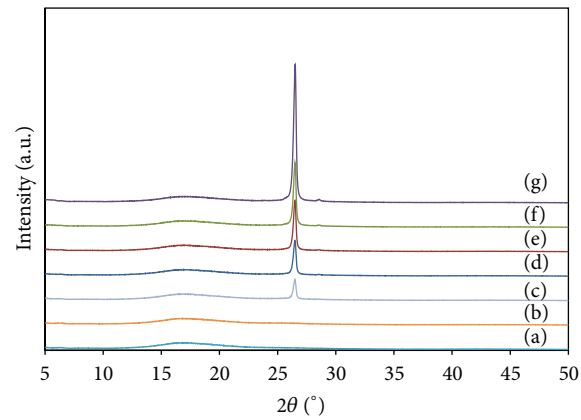

Figure 1: XRD patterns of the PC resin (a) and OGNP/MWCNT/PC nanocomposites at different OGNP loadings (phr): (b) 0, (c) 0.5, (d) 1.0, (e) 1.5, (f) 2.0, and (g) 5.0.

3.3. ESD Measurement. The Electronic Industry Association (EIA) specifies that the typical requirements for surface resistivity, tribocharge voltage, and decay times are 10^6–10^9 Ω/sq, less than 25 V, and less than 5 sec, respectively [39, 40]. The electrical properties such as electrical resistivity, tribocharge voltage, and decay times of OGNP/MWCNT/PC nanocomposites are presented in Table 1. Nanocomposites containing 2.0 wt% of MWCNTs and mixtures of 2.0 wt% of MWCNTs and 1.5–5.0 phr of OGNPs had tribocharge voltages, surface resistivities, and decay times within the ESD specification range. However, 2 wt% MWCNT/PC nanocomposites containing 0.5–1.0 phr of OGNPs did not meet the ESD requirements. At low levels of OGNPs, a conductive network of nanoplatelets was not generated, and ONGPs might obstruct the conductive network formation of MWCNTs as well, due to slight intercalation and dispersion degrees of OGNPs in the PC matrix. Du et al. [41] revealed that uniform distribution and low aggregation of carbon fillers in a polymer matrix caused a segregated network structure, resulting in a high conducting network formation at low filler loading. Moreover, the increase of OGNP contents did not have any significant effect upon the conductivity of MWCNT/PC

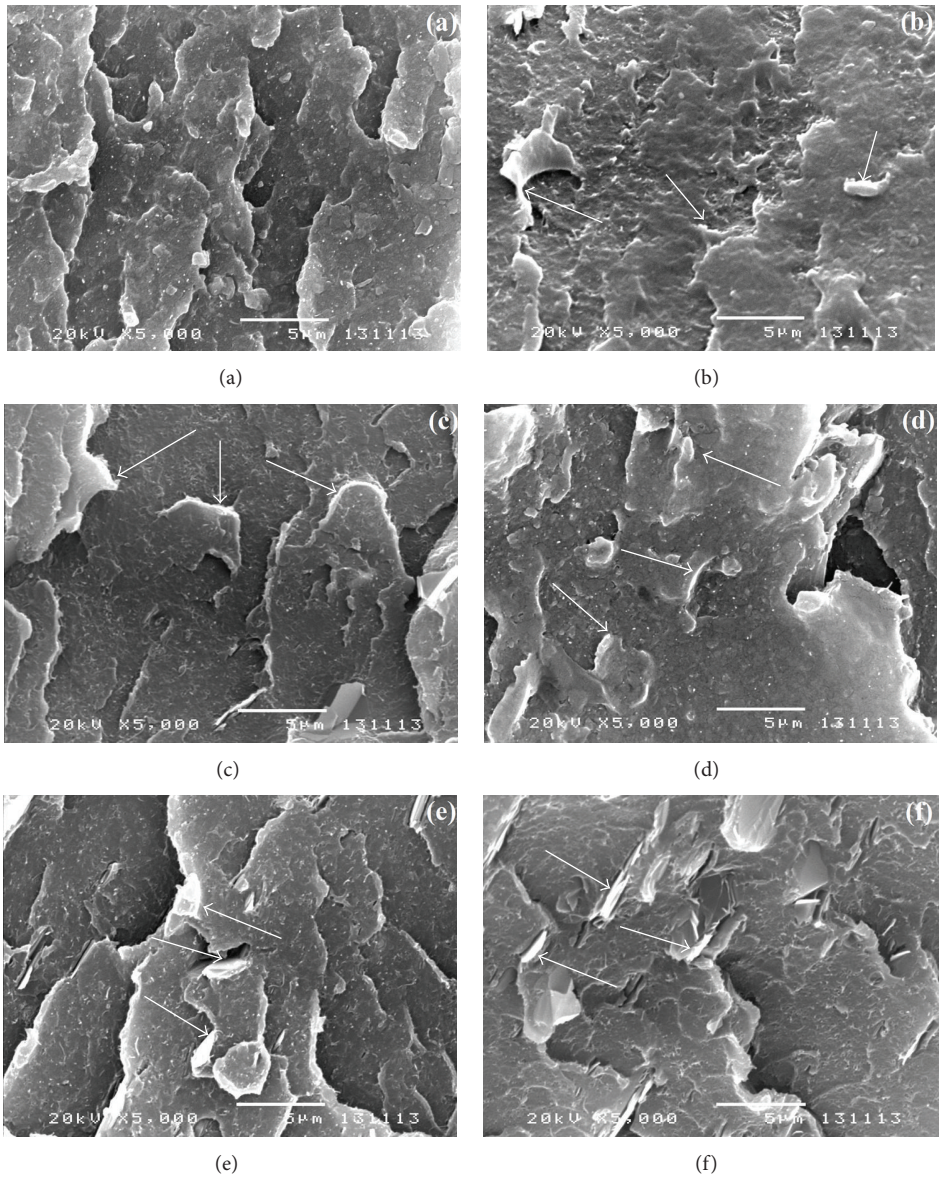

Figure 2: SEM images of fractured OGNP/MWCNT/PC nanocomposites at different OGNP content levels (phr): (a) 0, (b) 0.5, (c) 1.0, (d) 1.5, (e) 2.0, and (f) 5.0.

Table 1: ESD results of injection molded specimen based OGNP/MWCNT/PC nanocomposites at different OGNP contents.

OGNP content (phr)	Tribocharge voltage (V)	Surface resistivity (Ω/sq)		Decay time (sec) from 1000 V to 100 V		Compared result with EIA specification
		Point to point	Point to ground	Positive charge	Negative charge	
0.0	15	$3.92E + 10^7$	$1.84E + 10^8$	0.11	0.26	Passed
0.5	39	4.96×10^7	2.00×10^9	0.89	>5	Failed
1.0	46	5.27×10^7	1.15×10^9	0.52	>5	Failed
1.5	19	4.81×10^7	1.07×10^8	0.10	0.16	Passed
2.0	15	5.16×10^7	4.84×10^8	0.11	0.20	Passed
5.0	11	4.89×10^7	2.19×10^8	0.12	0.20	Passed

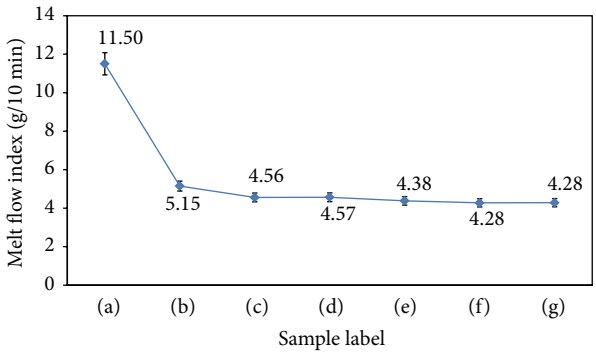

Figure 3: MFI results of (a) the PC resin and OGNP/MWCNT/PC nanocomposites at different OGNP contents (phr) at 260°C: (b) 0, (c) 0.5, (d) 1.0, (e) 1.5, (f) 2.0, and (g) 5.0.

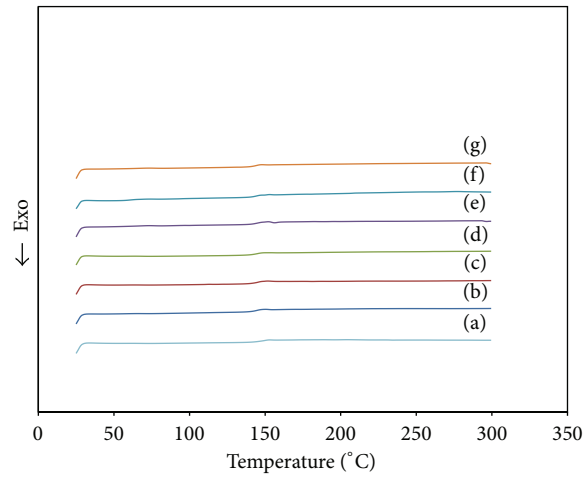

Figure 4: DSC curves of the PC resin (a) and OGNP/MWCNT/PC nanocomposites at different OGNP contents (phr): (b) 0, (c) 0.5, (d) 1.0, (e) 1.5, (f) (2.0), and (g) 5.0.

nanocomposites, since the resistivity change may still be within the steepness range (the percolation threshold) of the percolation curve. The percolation threshold indicates the critical amount of filler necessary to initiate a continuous conductive network, which varies from polymer to polymer for a given conductive filler type [1].

3.4. Melt Flow Index. The MFI of OGNP/MWCNT/PC nanocomposites decreased from 11.5 to 4.3 g/10 min and 5.2 to 4.3 g/10 min compared with the neat PC resin and the MWCNTs/PC nanocomposite, respectively (see Figure 3). However, the MFI of nanocomposites did not proportionally decrease with an increase in OGNP contents, due to poor dispersion and intercalation of OGNPs within the polymer matrix. A decrease in MFI indicated that the viscosity of the system increased with the addition of MWCNT and a combination of MWCNT/OGNP nanofillers. A transition from a liquid-like to a solid-like state occurred due to the formation of nanotube and nanoplatelet networks, which obstructed the motion of the polymer chains [42]. The presence of nanoplatelets generally causes a large energetic barrier for segmental motions of polymer chains in a confined space and thus increases flow activation energy. Furthermore, Barus et al. [43] revealed that strong interactions between the polymer matrix and fillers may cause greater activation energies of flow. The alignment of OGNP fillers during flow is thus not possible [44].

3.5. Thermal Properties. Thermal stability is very important for polymeric materials, as it is often the limiting factor both in processing and in end-use applications. Figure 4 shows the DSC heating thermogram of OGNP/MWCNT/PC nanocomposites at various OGNP concentrations. An apparent glass transition region was observed on the sample curves. The T_g values of PC nanocomposites were between circa 146°C and 147°C, as shown in Table 2. The T_g remained almost constant with the addition of MWCNTs and mixtures of MWCNTs and OGNPs, compared to the PC resin (T_g = 146°C). The heat capacity jump at the glass transition stages was quite constant with increase of OGNP contents, which was approximately 0.23–0.26 J g^{-1} °C^{-1} (see Table 2). It was reported in a previous study that the heat capacity jump at the glass transition stages strongly decreased with increasing OGNP contents [45]. It can thus be inferred that OGNPs restrict the motion of a significant fraction of polymer chain segments, preventing their participation in the glass transition process. However, chains that can participate in the glass transition do not affect the T_g.

Thermal degradation of the PC resin and PC nanocomposites with different weight fractions of OGNP was determined from weight loss measurements during heating. Figure 5 shows the TGA curves of OGNP/MWCNT/PC nanocomposites at different OGNP contents compared with the neat PC resin. The T_d of OGNP/MWCNT/PC nanocomposites changed significantly compared against that of pure PC (T_d = 493°C), as summarized in Table 2. Thermal degradation of the neat PC and its nanocomposites occurs as a single step process, with a maximum decomposition temperature at circa 520°C. The addition of OGNPs increased the thermal stability by around 30°C and 20°C compared against PC resin and MWCNT/PC nanocomposites, respectively. The T_d slightly changed as the dosage of OGNPs was increased. The improvement in the resistance to thermal degradation can be attributed to the hindered diffusion of volatile decomposition products within the nanocomposites, and this is strongly dependent upon the filler-polymer chain interactions [46]. OGNPs can be incorporated into a PC matrix by melt blending and without any noticeable degradation, since they exhibit sufficient thermal stability within the range where polymer processing is performed, namely, in the range of 240°C to 290°C.

3.6. Mechanical Properties. Mechanical properties of OGNP/MWCNT/PC composites measured using tensile strength and impact tests are presented in Figures 6–8. Tensile Young's modulus of nanocomposites was approximately in the range of 2.5–3.0 GPa, higher than that of the neat

Table 2: Thermal properties of OGNP/MWCNT/PC nanocomposites at different OGNP contents.

OGNPs content (phr)	T_{onset} (°C)	T_{mid} (°C)	T_{end} (°C)	Change in heat capacity $J\,g^{-1}\,°C^{-1}$	T_d (°C)
0.0	144.2	147.0	151.3	0.23	513
0.5	143.7	146.8	151.6	0.24	520
1.0	143.4	146.1	150.7	0.23	520
1.5	143.7	146.8	151.1	0.25	518
2.0	144.5	147.4	152.0	0.26	520
5.0	143.3	146.4	151.2	0.26	519

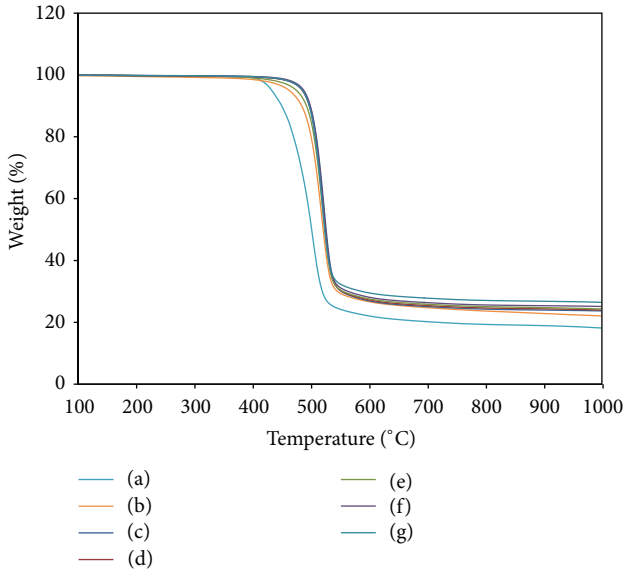

Figure 5: TGA curves of the neat PC (a) and OGNP/MWCNT/PC nanocomposites at different OGNP contents (phr): (b) 0, (c) 0.5, (d) 1.0, (e) 1.5, (f) (2.0), and (g) 5.0.

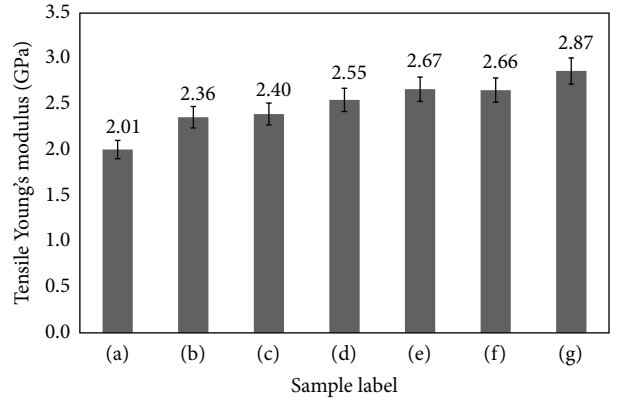

Figure 6: Tensile Young's modulus of (a) PC resin and OGNP/MWCNT/PC nanocomposites at different OGNP contents (phr): (b) 0, (c) 0.5, (d) 1.0, (e) 1.5, (f) 2.0, and (g) 5.0.

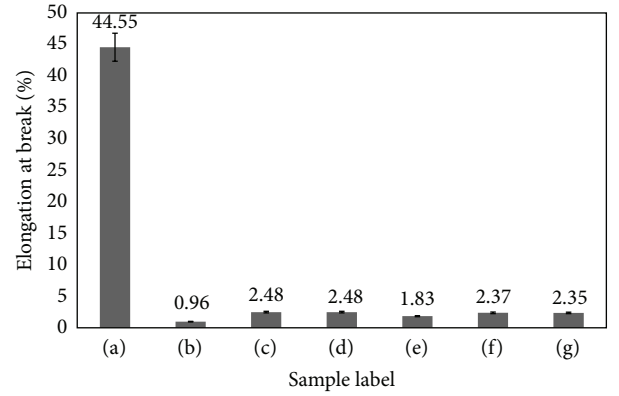

Figure 7: Elongation at break of (a) PC resin and OGNP/MWCNT/PC nanocomposites at different OGNP contents (phr): (b) 0, (c) 0.5, (d) 1.0, (e) 1.5, (f) 2.0, and (g) 5.0.

PC (2.0 GPa). Tensile Young's modulus of nanocomposites containing OGNP/MWCNT fillers was higher than that of the nanocomposite which merely had MWCNTs. Moreover, tensile Young's modulus tended to slightly increase as the contents of OGNPs were increased. The elongation at break of nanocomposites was more or less in the range of 1.0% to 2.5%, also much lower than that of the PC resin (at circa 45%). The elongation at break of nanocomposites containing MWCNT/OGNP hybrid fillers was higher than that of the nanocomposite containing only MWCNTs. However, the elongation at break slightly increased with an increase in OGNP concentrations.

The impact strength of nanocomposites was approximately in the range of between 5.0 and 7.5 J/m^2, which is much lower than that of the PC resin ($\cong$ 75 J/m^2). The impact strength of nanocomposites containing OGNP/MWCNT hybrid fillers was slightly higher than that of the MWCNT/PC nanocomposite, and the OGNP/MWCNT/PC nanocomposite showed little effect upon the mechanical properties compared with the nanocomposite containing only MWCNTs, due to poor dispersion and intercalation of OGNPs. The filler agglomeration can cause defects in the polymer matrix, leading to poor mechanical properties. Therefore, this implied that the effect of nanotubes (MWCNTs) was much larger than that of nanoplatelets (OGNPs), since the MWCNT master batch was prepared by the extrusion process, resulting in better dispersion of MWCNTs than that of OGNPs. It is well known that the modulus of fiber or particulate reinforced composites depends mainly upon the moduli and volume fractions of the composite constituents [47]. Unlike

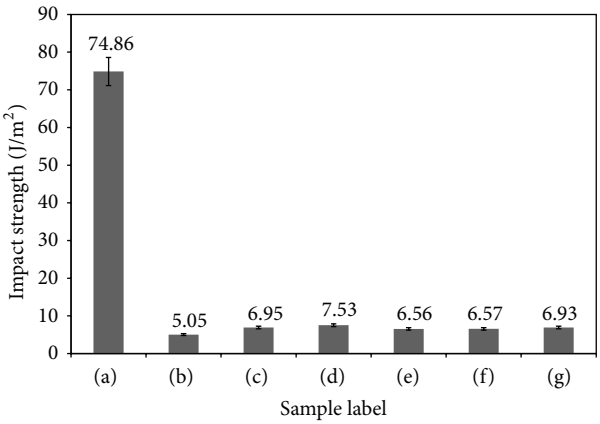

Figure 8: Impact strength of (a) PC resin and OGNP/MWCNT/PC nanocomposites at different OGNP contents (phr): (b) 0, (c) 0.5, (d) 1.0, (e) 1.5, (f) 2.0, and (g) 5.0.

the modulus, however, the strength of composites depends upon many factors in addition to the strengths and volume fractions of the composite constituents, amongst which the interfacial adhesion between the reinforcements and the matrix is a predominant factor [47]. In the case of nanofillers, the dispersion and intercalation or exfoliation, especially for graphenes and nanoclays, are also key factors which can impact upon the mechanical properties of nanocomposites [16, 23, 26, 42].

4. Conclusions

The mixtures of MWCNTs (2.0 wt%) and OGNPs at various concentrations (0.0–5.0 phr) were blended with the PC resin employing a melt compounding process and using a twin-screw corotating extruder. Electron microscopy and X-ray diffraction revealed poor dispersion and slightly intercalated morphology of OGNPs in the PC matrix, resulting in variations and insignificant improvements to nanocomposite properties. The oxygen-plasma treatment method might not be powerful enough to generate suitable functional groups on GNP to interact with the PC resin. The OGNP/MWCNT/PC nanocomposites containing 1.5–5.0 phr exhibited ESD properties within the specification range. The T_g of OGNP/MWCNT/PC nanocomposites changed insignificantly when compared to neat PC. The T_d value of the PC resin increased when MWCNTs and OGNPs were added to the system. The addition of OGNPs to PC matrix resulted in a decreased MFI, indicating an increase in melt viscosity. Tensile Young's modulus increased, whereas the impact strength and elongation at break both decreased when nanofillers were filled into the polymer matrix. The present study demonstrates that the OGNP/MWCNT/PC nanocomposite with low filler loadings is a promising material for the next generation of ESD composite applications, especially for injection moldable electronic packaging required to prevent electronic parts, devices, and finished products from electrostatic discharge. However, other surface modification methods on GNPs are required to improve their dispersion and intercalation into the PC matrix, such as oxidation and reduction processes.

Conflict of Interests

The authors declare that there is no conflict of interests regarding the publication of this paper.

Acknowledgment

The authors acknowledge the financial support from the 90th Anniversary of Chulalongkorn University Fund (Ratchadaphiseksomphot Endowment Fund).

References

[1] M. Narkis, G. Lidor, A. Vaxman, and L. Zuri, "New injection moldable electrostatic dissipative (ESD) composites based on very low carbon black loadings," *Journal of Electrostatics*, vol. 47, no. 4, pp. 201–214, 1999.

[2] Z. S. Petrović, B. Martinović, V. Divjaković, and J. B. Simendić, "Polypropylene-carbon black interaction in conductive composites," *Journal of Applied Polymer Science*, vol. 49, no. 9, pp. 1659–1669, 1993.

[3] P. G. Collins and P. Avouris, "Nanotubes for electronics," *Scientific American*, vol. 283, no. 6, pp. 62–69, 2000.

[4] J. Nilsson, A. C. Neto, F. Guinea, and N. Peres, "Electronic properties of graphene multilayers," *Physical Review Letters*, vol. 97, no. 26, Article ID 266801, 2006.

[5] M. Poot and H. S. J. van der Zant, "Nanomechanical properties of few-layer graphene membranes," *Applied Physics Letters*, vol. 92, no. 6, Article ID 063111, 2008.

[6] R. S. Ruoff and D. C. Lorents, "Mechanical and thermal properties of carbon nanotubes," *Carbon*, vol. 33, no. 7, pp. 925–930, 1995.

[7] A. A. Balandin, S. Ghosh, W. Bao et al., "Superior thermal conductivity of single-layer graphene," *Nano Letters*, vol. 8, no. 3, pp. 902–907, 2008.

[8] M. S. Dresselhaus, G. Dresselhaus, J. C. Charlier, and E. Hernández, "Electronic, thermal and mechanical properties of carbon nanotubes," *Philosophical Transactions of the Royal Society A: Mathematical, Physical and Engineering Sciences*, vol. 362, no. 1823, pp. 2065–2098, 2004.

[9] S. H. Jin, D. K. Choi, and D. S. Lee, "Electrical and rheological properties of polycarbonate/multiwalled carbon nanotube nanocomposites," *Colloids and Surfaces A: Physicochemical and Engineering Aspects*, vol. 313-314, pp. 242–245, 2008.

[10] M. Mahmoodi, M. Arjmand, U. Sundararaj, and S. Park, "The electrical conductivity and electromagnetic interference shielding of injection molded multi-walled carbon nanotube/polystyrene composites," *Carbon*, vol. 50, no. 4, pp. 1455–1464, 2012.

[11] Z. Spitalsky, D. Tasis, K. Papagelis, and C. Galiotis, "Carbon nanotube-polymer composites: chemistry, processing, mechanical and electrical properties," *Progress in Polymer Science*, vol. 35, no. 3, pp. 357–401, 2010.

[12] X. Li, S. Y. Wong, W. C. Tjiu, B. P. Lyons, S. A. Oh, and C. B. He, "Non-covalent functionalization of multi walled carbon nanotubes and their application for conductive composites," *Carbon*, vol. 46, no. 5, pp. 829–831, 2008.

[13] D. Aussawasathien and C. Teerawattananon, "Preparation and properties of woven carbon fiber mat-epoxy composites containing dispersed base-functionalized multi-walled carbon nanotubes," *Chiang Mai Journal of Science*, vol. 39, no. 3, pp. 524–539, 2012.

[14] S. H. Xie, Y. Y. Liu, and J. Y. Li, "Comparison of the effective conductivity between composites reinforced by graphene nanosheets and carbon nanotubes," *Applied Physics Letters*, vol. 92, no. 24, Article ID 243121, 2008.

[15] M. El Achaby, F.-E. Arrakhiz, S. Vaudreuil, A. El Kacem Qaiss, M. Bousmina, and O. Fassi-Fehri, "Mechanical, thermal, and rheological properties of graphene-based polypropylene nanocomposites prepared by melt mixing," *Polymer Composites*, vol. 33, no. 5, pp. 733–744, 2012.

[16] W. Li, A. Dichiara, and J. Bai, "Carbon nanotube-graphene nanoplatelet hybrids as high-performance multifunctional reinforcements in epoxy composites," *Composites Science and Technology*, vol. 74, pp. 221–227, 2013.

[17] J. Y. Yi and G. M. Choi, "Percolation behavior of conductor-insulator composites with varying aspect ratio of conductive fiber," *Journal of Electroceramics*, vol. 3, no. 4, pp. 361–369, 1999.

[18] D. Zhu, Y. Bin, and M. Matsuo, "Electrical conducting behaviors in polymeric composites with carbonaceous fillers," *Journal of Polymer Science Part B: Polymer Physics*, vol. 45, no. 9, pp. 1037–1044, 2007.

[19] S. Stankovich, D. A. Dikin, G. H. B. Dommett et al., "Graphene-based composite materials," *Nature*, vol. 442, no. 7100, pp. 282–286, 2006.

[20] T. Ramanathan, A. A. Abdala, S. Stankovich et al., "Functionalized graphene sheets for polymer nanocomposites," *Nature Nanotechnology*, vol. 3, no. 6, pp. 327–331, 2008.

[21] S. Ansari and E. P. Giannelis, "Functionalized graphene sheet-Poly(vinylidene fluoride) conductive nanocomposites," *Journal of Polymer Science, Part B: Polymer Physics*, vol. 47, no. 9, pp. 888–897, 2009.

[22] G. Eda and M. Chhowalla, "Graphene-based composite thin films for electronics," *Nano Letters*, vol. 9, no. 2, pp. 814–818, 2009.

[23] H. Kim and C. W. Macosko, "Processing-property relationships of polycarbonate/graphene composites," *Polymer*, vol. 50, no. 15, pp. 3797–3809, 2009.

[24] Y. Zhan, J. Wu, H. Xia, N. Yan, G. Fei, and G. Yuan, "Dispersion and exfoliation of graphene in rubber by an ultrasonically-assisted latex mixing and in situ reduction process," *Macromolecular Materials and Engineering*, vol. 296, no. 7, pp. 590–602, 2011.

[25] J. Aalaie, A. Rahmatpour, and S. Maghami, "Preparation and characterization of linear low density polyethylene/carbon nanotube nanocomposites," *Journal of Macromolecular Science Part B: Physics*, vol. 46, no. 5, pp. 877–889, 2007.

[26] J. R. Potts, D. R. Dreyer, C. W. Bielawski, and R. S. Ruoff, "Graphene-based polymer nanocomposites," *Polymer*, vol. 52, no. 1, pp. 5–25, 2011.

[27] H. Kim, A. A. Abdala, and C. W. Macosko, "Graphene/polymer nanocomposites," *Macromolecules*, vol. 43, no. 16, pp. 6515–6530, 2010.

[28] J.-L. Li, K. N. Kudin, M. J. McAllister, R. K. Prud'homme, I. A. Aksay, and R. Car, "Oxygen-driven unzipping of graphitic materials," *Physical Review Letters*, vol. 96, no. 17, Article ID 176101, 2006.

[29] N. P. Zschoerper, V. Katzenmaier, U. Vohrer, M. Haupt, C. Oehr, and T. Hirth, "Analytical investigation of the composition of plasma-induced functional groups on carbon nanotube sheets," *Carbon*, vol. 47, no. 9, pp. 2174–2185, 2009.

[30] J. Yun, J. S. Im, and H.-I. Kim, "Effect of oxygen plasma treatment of carbon nanotubes on electromagnetic interference shielding of polypyrrole-coated carbon nanotubes," *Journal of Applied Polymer Science*, vol. 126, no. 2, pp. E39–E47, 2012.

[31] J. Rodríguez-Hernández, "Wrinkled interfaces: taking advantage of surface instabilities to pattern polymer surfaces," *Progress in Polymer Science*, 2014.

[32] T. S. Dunn, D. Montgomery, J. P. O'connell, and J. L. Williams, "Heparinization of plasma treated surfaces," US Patents 4613517, 1986.

[33] L.-A. O'Hare, S. Leadley, and B. Parbhoo, "Surface physicochemistry of corona-discharge-treated polypropylene film," *Surface and Interface Analysis*, vol. 33, no. 4, pp. 335–342, 2002.

[34] M.-J. Wang, Y.-I. Chang, and F. Poncin-Epaillard, "Acid and basic functionalities of nitrogen and carbon dioxide plasma-treated polystyrene," *Surface and Interface Analysis*, vol. 37, no. 3, pp. 348–355, 2005.

[35] R. Sengupta, M. Bhattacharya, S. Bandyopadhyay, and A. K. Bhowmick, "A review on the mechanical and electrical properties of graphite and modified graphite reinforced polymer composites," *Progress in Polymer Science (Oxford)*, vol. 36, no. 5, pp. 638–670, 2011.

[36] B. Li and W.-H. Zhong, "Review on polymer/graphite nanoplatelet nanocomposites," *Journal of Materials Science*, vol. 46, no. 17, pp. 5595–5614, 2011.

[37] R. J. Zaldivar, J. P. Nokes, P. M. Adams, K. Hammoud, and H. I. Kim, "Surface functionalization without lattice degradation of highly crystalline nanoscaled carbon materials using a carbon monoxide atmospheric plasma treatment," *Carbon*, vol. 50, no. 8, pp. 2966–2975, 2012.

[38] H. Wu and L. T. Drzal, "Graphene nanoplatelet-polyetherimide composites: revealed morphology and relation to properties," *Journal of Applied Polymer Science*, vol. 130, no. 6, pp. 4081–4089, 2013.

[39] D. Aussawasathien and C. Teerawattananon, "Deposition of aluminum oxide-doped zinc oxide transparent nano-films on glass substrates for electrostatic discharge applications," *Materials Science in Semiconductor Processing*, vol. 15, no. 3, pp. 293–300, 2012.

[40] A. Poosala, D. Aussawasathien, D. Pentrakoon, and A. Chandrachai, "The front end in anti-electrostatic discharge for product innovation development: polycarbonate/graphene composite," *International Journal of Innovative Research in Science, Engineering and Technology*, vol. 2, no. 9, pp. 4724–4734, 2013.

[41] J. Du, L. Zhao, Y. Zeng et al., "Comparison of electrical properties between multi-walled carbon nanotube and graphene nanosheet/high density polyethylene composites with a segregated network structure," *Carbon*, vol. 49, no. 4, pp. 1094–1100, 2011.

[42] J. Aalaie, A. Rahmatpour, and S. Maghami, "Preparation and characterization of linear low density polyethylene/carbon nanotube nanocomposites," *Journal of Macromolecular Science, Part B: Physics*, vol. 46, no. 5, pp. 877–889, 2007.

[43] S. Barus, M. Zanetti, P. Bracco, S. Musso, A. Chiodoni, and A. Tagliaferro, "Influence of MWCNT morphology on dispersion and thermal properties of polyethylene nanocomposites," *Polymer Degradation and Stability*, vol. 95, no. 5, pp. 756–762, 2010.

[44] S.-Y. Gu, J. Ren, and Q.-F. Wang, "Rheology of poly (propylene)/clay nanocomposites," *Journal of Applied Polymer Science*, vol. 91, no. 4, pp. 2427–2434, 2004.

[45] Y. Zhan, J. Wu, H. Xia, N. Yan, G. Fei, and G. Yuan, "Dispersion and exfoliation of graphene in rubber by an ultrasonically-assisted latex mixing and in situ reduction process," *Macromolecular Materials and Engineering*, vol. 296, no. 7, pp. 590–602, 2011.

[46] M. El Achaby, F.-E. Arrakhiz, S. Vaudreuil, Q. A. El Kacem, M. Bousmina, and O. Fassi-Fehri, "Mechanical, thermal, and rheological properties of graphene-based polypropylene nanocomposites prepared by melt mixing," *Polymer Composites*, vol. 33, no. 5, pp. 733–744, 2012.

[47] J. Li, P.-S. Wong, and J.-K. Kim, "Hybrid nanocomposites containing carbon nanotubes and graphite nanoplatelets," *Materials Science and Engineering A*, vol. 483-484, no. 1-2, pp. 660–663, 2008.